International Journal of Lakes and Rivers.
ISSN 0973-4570 Volume 17, Number 2 (2024), pp. 75-108

http://www.ripublication.com/ijlr.htm

# The Effects of Soil Location Sampling for River Regime Analysis: A Case Study of Plumbon River, Semarang City

**Eka Oktariyanto Nugroho[1,2*], Yadi Suryadi[1,2], Renaldy Andrean[2], Arno Adi Kuntoro[1,2], Indratmo Soekarno[1,2], Dayu Apoji[3], Dhemi Harlan[1,2], Widharta Kusuma[2]**

*[1] Water Resources Engineering Research Group, Civil Engineering Study Program, Faculty of Civil and Environmental Engineering, Bandung Institute of Technology, Indonesia*
*[2] Water Resources Management Master's Program, Bandung Institute of Technology, Indonesia*
*[3] Geotechnical Engineering Research Group, Civil Engineering Study Program, Faculty of Civil and Environmental Engineering, Bandung Institute of Technology, Indonesia*

**Abstract.**

River is a product of natural geological processes where the process of erosion, sediment transport, and deposition become the main catalysts that shape the river landscapes. In hydraulics, regime means neither scoured nor filled, which is not possible in practice. A concept to create the interrelationship between flow, sediment transport, channel resistance, and bank stability was developed in the late nineteenth century called the Regime Theory. It is used to predict the shape, size, and slope of a channel that is as regime as possible. The methods used are mentioned as follows: Lacey, Blench, Generalized Regime, Process-Based Regime, Kellerhals, Griffiths, and Hey&Thorne. Across those methods, dominant flow and grain size stand as the main variables. Problem arises in grain size variable as most studies prefer to use mean finer percentage diameter size and center bed sample location. This paper presents a study on applying regime dimensioning in Plumbon River by changing the finer percentage of soil samples and different soil specimen spots to learn the effect of grain sizes on regime dimensions. The study concludes that: (1) Interpolation between observed data has the best result to fill unobserved data; (2) Plumbon River's current state is the closest to Hey&Thorne for width and Kellerhals for depth and slope; (3) Width becomes the dimension that is the least unstable, followed by slope and depth; (4) Against finer percentage, width and slope are directly proportional while depth is reversely proportional; (5) Three samples' representation per each river slope classification results best; and (6) Moving soil specimen spots to the left or right while still being inside the bank stations are allowed for only width dimensioning.

**Keywords:** Grain size interpolation, Plumbon River, regime dimensioning, soil finer percentage, soil specimen spot.

## 1. Introduction

Streams and rivers are products of natural geological processes, fluvial dynamics, and human modifications. The process of erosion, sediment transport, and deposition become the main catalysts that shape the river landscapes on Earth [1]. In hydraulics, regime channel means neither scoured nor filled. In practice, a regime state is not possible because the alluvium channel is constructed based on continuous scouring and filling in both beds and banks. The regime can be understood as the state of equilibrium between the amount of scour and the amount of fill in a long-term perspective to be satisfied.

The discussion of regime's definition was started by Blench in 1952 [2], but was critiqued by Stevens and Nordin in 1987 [3]. In between that, Wolman in 1955 [4] stated some key points that can summarize the whole discussion on regime, regimen, equilibrium, and poised as follows:

(1) They all imply stability with each different certain amount in time.

(2) They all imply a set of adjustments that is flexible to be changed in the channel's changes.

(3) They all have no fixed parameter or criteria used to judge the stability of the given stream neither in regime, poised, exhibit, nor average equilibrium.

(4) They all do not imply that the adjustments in the cross section's shape will be more influential in its stability state compared to slope adjustment, or vice versa.

These points were further strengthened by Schumm (1984) [27] and Thorne (1999) [28] who illustrated how a channel is most likely to evolve throughout time, with an unknown duration as shown in Fig. 1. Most channels back in time started in a condition named Pre-adjustment. The Pre-adjustment is in regime in which processes of degradation and aggradation may occur between spring and fall, but it will remain consistent year to year in balance. Through time, a channel will degrade, widen, and aggrade, until an uncertain time in the future when it will reach a condition named Quasiequilibrium, which is a new dynamic equilibrium and once again is in a regime state. These processes are believed to be repeated again and again.

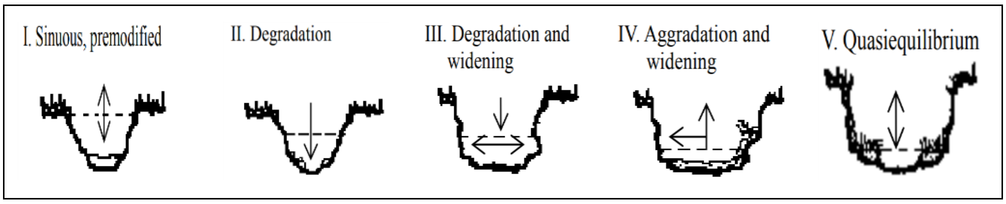


**Figure 1.** Channel evolution model through time. [27-28]

Ackers in 1992 [5] serves a discussion about the description of river's stability that needs to be described in the boundary of the different scales. The first one is the ripple scale, which will be directly related to the particle size in micro-scale. The second is at the scale of dunes and bars, where it will be directly related to channel depth. The third is at the scale of shoals and meanders, and it will be directly related to channel width in macro-scale. Slope, on the other hand, is a long-sectional part outside cross-sectional's depth and width that becomes the base output of regime theory.

Regime dimensioning was first developed in the late nineteenth century in India to design and operate extensive irrigation canal systems. The dependent variables are width, depth, and slope, while dominant discharge, bed gradation, and sediment-inflow concentration become the independent variables. At first, the dependents that were determined using regression analysis were only applicable to low-energy river systems where the discharge is relatively uniform with time and has low sediment transport. In number, Froude is normally less than 0.3 [6]. Figure 2 illustrates the changes upon a channel by cross-sectional, which are either widening or narrowing for width and degradation or aggradation for depth. Figure 3 illustrates the changes upon a channel by long-sectional, which varies in slope changes throughout an unknown duration of time that also causes the change in river shape.

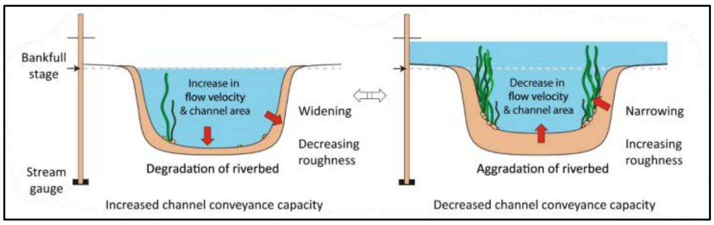


**Figure 2.** Changes in cross-sectional. [29]

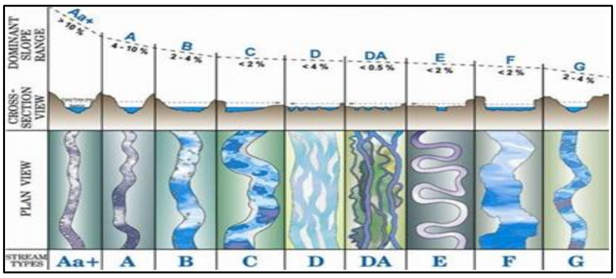


**Figure 3.** Changes in long sectional. [30]

Following the application in India, studies on the theory started appearing and developing. The main concept of regime in an alluvium channel will fully depend on the interrelationship between flow, sediment transport, channel resistance, and bank stability. This interrelationship will be the determinant factor of the channel shape and stability through empirically dimensioning the depth, width, and slope. The empirical measurements were done on a channel resulting in observed data used for fitting in creating the empirical equations. Fitting is primarily related to discharge, and variably related to sediment size. [3]

Throughout some past studies about the application of regime dimensioning in rivers [31-33], some similarities become the main concerns in this study.

(1) One, the use of regime dimensioning is only to compare the closest method of regime dimension to the current state's dimension. This is normally done by comparing only the slope dimension, and further proceeding by designing the width and depth based on the chosen method.

(2) Two, an assessment of the instability of a studied cross section within regime dimensioning is never described in a quantitative description. The conclusion of an unstable channel based on the current state's inability to reach the regime dimension is not enough. The ability to explain the value of reliability or the risk of river safety is absent.

(3) Three, in some regime methods that use the variable of grain size, the use of only mean bed gradation size becomes a problem. In practice, there might be a condition where the center bed in a channel is inaccessible. In other conditions, there might be an analysis that is soon to be done by using secondary grain size data, which may not provide the mean gradation size.

In most practices, river operations are often limited by resources such as time, costs, and manpower. This limitation causes an effort of data collection simplification to minimize the use of resources while still producing the most. The simplification is done in the form of minimalizing data samples by assuming that in an expanse of the studied river, the location of three points (most upstream, middle stream, and most downstream) would be able to represent the whole river's condition. This study divides Plumbon River into six different classes by its slope. The idea is to propose a new standard of data samples' simplification, by substituting the locations all over these slope sections.

Plumbon River located in Semarang City, Central Java, Indonesia, is a river with a total length of 19.8 kilometers where natural states are still maintained in most of its sections. This study will be applying and averaging seven different methods of regime theory in Plumbon River including Lacey [8], Blench [9], Generalized Regime [10], Process-Based Regime [11], Kellerhals [12], Griffiths [13], and Hey&Thorne [14]. Based on the concerns mentioned in the previous paragraphs, the objectives of this study are:

(1) Analyzing ways to fill unobserved soil data based on known data

(2) Finding the most suitable method for the river's current state in each dimension

(3) Averaging regime dimensions from more than one method

(4) Quantifying the dimensions in the present state to regime state

(5) Analyzing the correlation between river slope classification to regime ratios

(6) Analyzing how different finer percentages and soil sample spots with different grain sizes in the same cross-section will affect the results.

## 2. Method and Material

### 2.1 Regime Dimensioning Methods

#### 2.1.1 Lacey

The regime dimensioning by Lacey in 1929 [18] started as the continuation of observation by Kennedy in 1895 [19] in Bari Doah, Punjab, India. The observation is done to create an empirical relation between averaged cross-sectional velocity to its average flow depth over the bed. The condition on the site is as listed, flow ranging from 26-1700 feet cube per second, averaged depth of 2.2-7.0 feet, and Froude number below 0.3. Lacey developed the existing parameters and results into three different functions, each representing velocity, wetted perimeter, and slope. Wallingford and Ackers in 1964 [8] in Hydraulic Research Station continued and simplified what Lacey had done to be applicable in more rivers, with equations stated in Table 2.

#### 2.1.2 Blench

Malhotra in 1939 [7] introduced factors named $F_B$ and $F_S$, each defining the factor of bed and sides to isolate the impact of bed material with alluvium formation in the side banks. The slope function is normalized as friction factor within a function for width-based Reynold number. As the result of Blench's experiment in 1951 [9], the relation of both these factors correlated with mean bed material diameter (Eq (1, 2)) creates the equations in Table 2.

$$F_B=1.9\sqrt{D_{50}} \quad \textbf{(1)}$$

$$\frac{w}{d}=v\frac{F_B}{F_S} \quad \textbf{(2)}$$

Where,

w = Channel width (m)

d = Channel depth (m)

v = Water kinematic viscosity

$F_B$ = Bed factor

$F_S$ = Side factor

### 2.1.3 Generalized Regime

Lacey and Pemberton in 1972 [20] conducted research to prove $v/R^{0.5}$ and $R^{0.5}/S$ were varied from one system to the others, independent to the flow and in a set of sedimentology system. Using field observation method, a special relationship between a multiplier constant to dominant flow to bed and bank materials is obtained. The coefficients are established as follows in Table 1, concluded with the equations as stated in Table 2.

**Table 1.** Generalized regime coefficients. [20]

| Coefficient | Sand bed and sand banks | Sand bed and cohesive banks | Cohesive bed and cohesive banks |
|---|---|---|---|
| C1 | 3.3 | 2.51 | 2.12 |
| C2 | 0.37 | 0.43 | 0.51 |
| C3 | 1.22 | 1.08 | 1.08 |
| C4 | 13.9 | 16.1 | 16 |
| C5 | 6.5 | 4.3 | 3 |

### 2.1.4 Process-Based Regime

The equations of sediment transport and alluvial resistance functions by Ackers in 1983 [21] and 1988 [22] are based on the principles of dimensions consistency, similarity, bed material transport, and turbulent suspensions' mechanics. Simons and Alberton in 1960 [23] analyzed channel dimensioning using the functions of sediment transport and resistance, but with the complex estimation of channel width, that is defined with experimented constant based on bed sediments and dominant flow. A problem occurred when the constant obtained was different from what Bakker in 1986 [24] concluded. This created an extended discussion throughout the years, from one research to another. The simplification of these equations was best introduced by Kondap and Garde in 1979 [11], as stated in Table 2.

### 2.1.5 Kellerhals

Kellerhals in 1967 [12] analyzed the roughness, slope, and discharge-decreasement on twelve different channels, including seven of which are gravel dominant and five of which done in laboratories. The conditions given are as follows, with gravel ranging from 0.5-18 inches and a dominant flow of 1-100.000 feet cube per second. Through those observations, equations of regime dimension are concluded as stated in Table 2.

### 2.1.6 Griffiths

Using statistical analysis, Griffiths in 1980 [13] derived a hydraulic geometry relation between width, depth, velocity, slope, suspended sediment concentration, and hydraulic roughness (Darcy-Weisbach) in gravel-dominant rivers in New Zealand. The flow analyzed is averaged yearly flow, with the conclusion of equations stated in Table 2.

### 2.1.7 Hey&Thorne

Using sixty-two data of "stable" rivers with graveled beds in United Kingdom, Hey and Thorne in 1986 [14] derived equations from variables such as follows to regime dimension equations stated in Table 2.

(1) Average width

(2) Mean depth

(3) Maximum depth

(4) Average slope

(5) Average bankfull reach velocity

(6) Wetted perimeter

(7) Hydraulic radius in bankfull discharge state

(8) Bed sediment load transport

(9) Median sediment diameter

(10) Shear strength of bank material

(11) Standard deviation of log-normal size frequency distribution

(12) Index of vegetation density

**Table 2:** Methods and equations for regime dimensioning. [8-14]

| **Theory** | **Equation** | | |
|---|---|---|---|
| | **Width (w)** | **Depth (d)** | **Slope (S)** |
| Lacey [8] | $3.6Q^{0.42}$ | $0.28Q^{0.42}$ | $f_L{}^{1,67}/1{,}79Q^{1/6}$ |
| Blench [9] | $(F_B.Q/F_S)^{0.5}$ | $(F_S.Q/F_B{}^2)^{1/3}$ | $F_B{}^{5/6}F_S{}^{1/12}Q^{-1/6}K^{-1}$ |
| Generalized Regime [10] | 0.9P | 1.73R | $((nQ)/(1.486A(R^{2/3}))^2$ |
| Process-Based Regime [11] | $Q^{0.548}D^{-0.0235}$ | $Q^{0.384}D^{-0.1276}$ | $fm^{5/3}/1.83Q^{1/6}$ |
| Kellerhals [12] | $1.8Q^{0.5}$ | $0.166Q^{0.4}ks^{-0.12}$ | $0.12Q^{-0.4}ks^{0.92}$ |
| Griffiths [13] | $7.09Q^{0.48}$ | $0.21Q^{0.43}$ | $0.02Q^{-0.49}$ |
| Hey&Thorne [14] | $3.67Q^{0.45}$ | $0.22Q^{0.37}D_{50}{}^{-0.11}$ | $0.008Q^{-0.31}D_{50}{}^{0.71}$ |

### 2.2 Dominant Discharge

Regime state needs to be seen in a macro-scale model, which is assessed in a long-term channel development (over 10 years or longer). The consideration sides with the dominant discharge to consider the long-term changes of the averaged channel's dimensions. Although widely varying flows happen in natural channels, only a certain range of flow called formative flow impacts the stream size and geometry. It is called formative because, at this discharge, the active changes in morphologic stability are at their highest through bank erosion and sediment movement. [6]

Bankfull discharge is defined as the flow that creates a maximum water level state within its capacity without causing any flooding [15]. This flow is often considered as the dominant flow that generates the same regime channel dimension as the natural sequences of flow [6]. The value of bankfull discharge varies from one river to the others, and one section in the same system to the others. Nixon in 1959 [16] states that in the studied watersheds, bankfull flow will occur for several days a year with approximately the same value as the mean annual flow. This strengthens the use of bankfull discharge for analyzing regime dimensioning, as it concludes how this flow controls the generalization of meander length and diminishment of sediment transport [17].

### 2.3 Grain Size

As stated in the introduction, Ackers in 1992 [5] serves a discussion about the description of river's stability that needs to be described in the boundary of the different scales. The first one is the ripple scale, which will be directly related to the particle size in micro-scale. Throughout the methods stated in Table 2, five out of seven methods use grain size as its main variable. Some of them state the use of $D_{50}$, or mean bed material diameter, and some give the flexibility to choose among the finer percentage to adjust the conservativeness in design. The relations in equations show that grain size has either directly or reversely proportional relation with regime dimensions, meaning as one increases so is the others, and vice versa [6].

### 2.4 Error Checking

#### 2.4.1 Root Mean Squared Error (RMSE)

Root Mean Squared Error (RMSE) is a standard metric to evaluate certain models between a pair of observation data and model data [34]. As its name implies, RMSE is the square root of Mean Squared Error (MSE) test that yields a metric that represents normally distributed errors. Chai and Draxler in 2014 [35] mention that RMSE is really good and standardized to measure model performance regarding meteorology, air quality, and climate research studies. According to studies, it results and translates better for conditions regarding nature more than MSE (and MAE) and is superior in statistics. The formula for RMSE is shown as follows:

$$RMSE = \sqrt{\frac{1}{n}\sum_{i=1}^{n}(y_i - \hat{y}_i)^2} \quad \textbf{(3)}$$

Where,

n = Number of data

$y_i$= Sample of *n* observations

$\hat{y}_i$ = Sample of *n* model predictions

### 2.4.2 Mean Absolute Deviation (MAD)

Mean Absolute Deviation (MAD) is a method used for evaluating results by forecasting methods by using the sum of simple mistakes [36]. It measures the accuracy of a prediction from its averaged alleged error, or the absolute value of each error. Moon in 2011 [37] and Leys in 2013 [38] concluded that MAD is really good at measuring prediction errors between a pair of data with the same unit. The formula for MAD is shown as follows:

$$\text{MAD}=\frac{\sum |y_i - y_t|}{n} \quad \textbf{(4)}$$

Where,

n = Number of data

$y_i$ = Sample of *n* observations

$y_t$.= Sample of *n* model predictions

2.4.3 Mean Absolute Percentage Error (MAPE)

Mean Absolute Percentage Error (MAPE) is a method used to validate a set of forecasted data against observation data, and is done by calculating the absolute error in each period divided by the observation values that are evident for that period [36]. It is normally written in percentages, and is at its best when the size of a prediction variable is significant in evaluating the accuracy of a prediction [39-40]. All in all, MAPE defines the indication of how much error is in the predicted data compared to the real values, with the formula as follows:

$$\text{MAPE} = \frac{\frac{\sum |y_i - y_t|}{y_i}}{n} \times 100\% \quad \textbf{(4)}$$

Where,

n = Number of data

$y_i$ = Sample of *n* observations

$y_t$ = Sample of *n* model predictions

# 3. Data and Methodology

## 3.1 Data Collection

The data used in this study are primarily obtained and listed as follows: (a) River's Geometries Data measured in August 2022; and (b) Soil specimens in five different spots in each cross-section surveyed, including left and right bank spots, left and right bank toe spots, and bed spot (Fig. 4). The soil specimens were brought to the laboratory for grain size analysis, with the outputs of sieve analysis and finer percentage in each diameter size classification (Fig. 7).

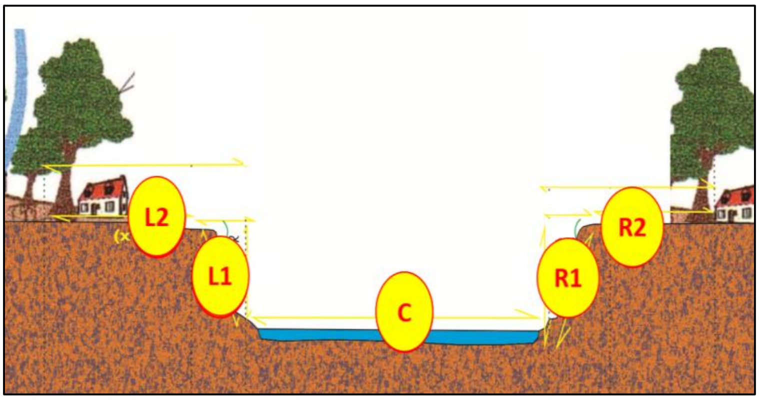


**Figure 4.** Soil specimen spots.

## 3.2 Hydraulic Analysis

As stated in the introduction, Plumbon River has a total length of approximately 19.8 kilometers, which is analyzed every 100 meters. To help the process of calculating the dominant discharge, or bankfull discharge, software specializing in hydraulic modeling named HEC-RAS is used. The process is to use the feature of 1-D Modelling, run a steady flow high enough to fill all the set banks in every cross-section and be taken as outputs for calculating the bankfull discharge. To accommodate the length, the river is divided into six different sections based on its slope levels. This will help distribute the loads intended to fill the geometries in every special location. Table 3 and Fig. 5 shows the river classification, and Fig. 6 shows the illustration of wetted areas calculation with HEC-RAS. [25]

**Table 3:** River slope classification.

| **No** | **Code** | **Slope (%)** | **Watershed Area ($km^2$)** |
|---|---|---|---|
| 1 | R1 | 6.58 | 55.93 |
| 2 | R2 | 0.90 | 22.98 |
| 3 | R3 | 4.32 | 18.63 |
| 4 | R4 | 1.41 | 17.89 |
| 5 | R5 | 0.37 | 0.81 |
| 6 | R6 | 0.05 | 0.72 |

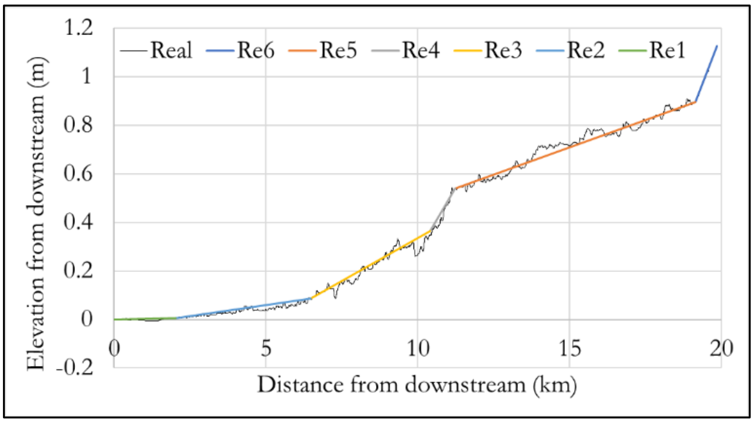


**Figure 5.** River long section slope classification.

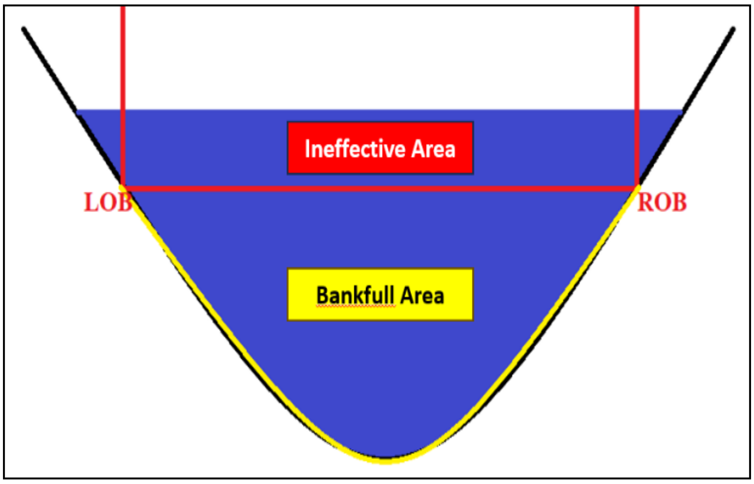


**Figure 6.** Illustration of bankfull area output from hydraulic analysis with HEC-RAS.

With HEC-RAS, the outputs are channel's area, wetted perimeter, inverted slope, and Manning's roughness number. The problem here lies in the channel's area where it does not represent only the flow bounded by the set bank stations. To produce the wetted area intended, further steps are needed with equations such as the following:

$$A_{BF}=A_{CH}-A_{IF} \quad \textbf{(6)}$$

$$A_{IF}=Sta(ROB-LOB)El(WSE-min(LOB:ROB)) \quad \textbf{(7)}$$

Where,

$A_{BF}$ = Bankfull area ($m^2$)

$A_{CH}$ = Channel's flow area ($m^2$)

$A_{IF}$ = Ineffective flow area ($m^2$)

$LOB_{ST}$ = Left bank station (m)

$ROB_{STA}$ = Right bank station (m)

WSE = Water elevation (m)

$LOB_{El}$ = Left bank elevation (m)

$ROB_{El}$ = Right bank elevation (m)

### 3.3 Grain Size Analysis

As shown in Fig. 4, each cross-section in this study will have five different samples to be analyzed in the laboratory to get through sieve analysis. However, due to the limited resources on the field survey in 2022, only 74 out of 195 cross-section samples were taken and brought for further tests (Fig. 7).

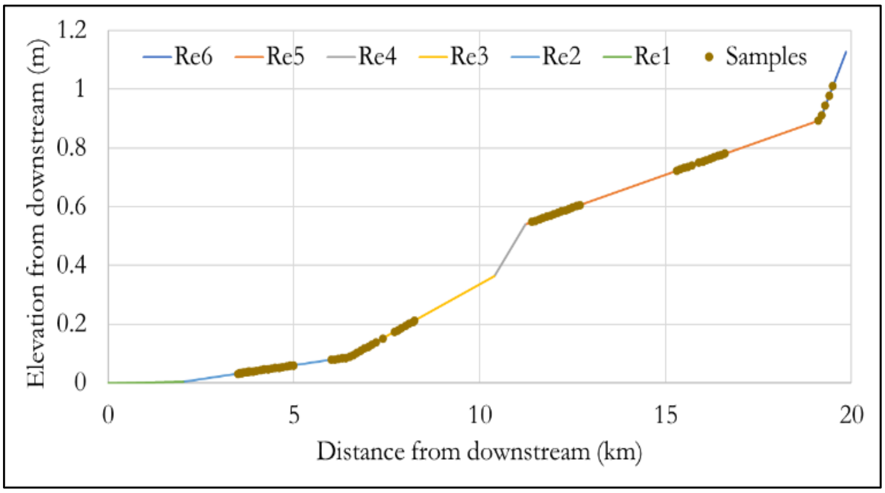


**Figure 7.** Soil sample locations on long section.

Because the application of regime dimensioning will be done in cross-sectional, missing data in between in Fig. 7 need to be filled in. There are three approaches to do this task:

(1) The first approach is to interpolate linearly from the whole data's trendline, called "Linear Interpolation".

(2) The Second approach is to interpolate linearly from in between two known data, called "Forecast Interpolation".

(3) The third approach is to interpolate linearly from the relation of shear stress and $D_{50}$, called "Shear Stress Correlation Interpolation".

### 3.4 Regime Dimensioning

Regime dimensioning is done to predict the regime state of river's shape and size, exclusively the variable of width and depth in cross-sectional and slope in long-sectional. This study refers to seven different methods mentioned in **Sub-unit 2.3**, with all of them having the dominant discharge as its main variable and only five of them having grain size as the other main variable (Table 2)

## 4. Result and Discussion

### 4.1. Grain Size from Sieve Analysis

The sieve analysis result is shown the Fig. 8 with the example of most upstream cross sections. For the first part of the study, $D_{50}$ is taken in each graph by interpolating the 50% value in the y-coordinate's percentage finer. The results for each specimen spot (L2 to R2) are also shown as follows. Table 4 results in the averaged mean grain diameter and its soil type based on the size.

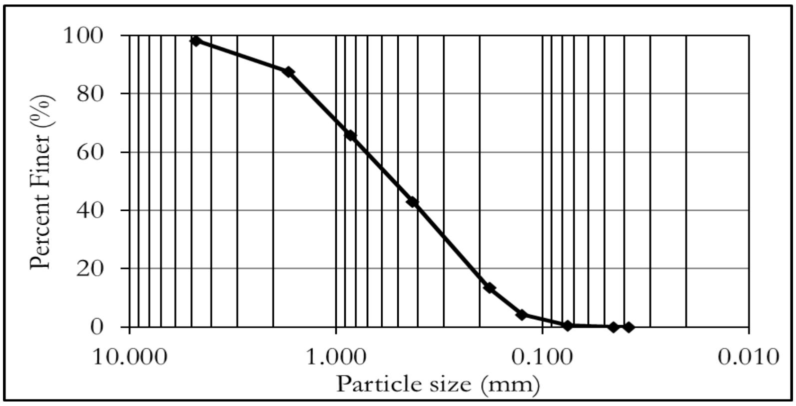


**Figure 8.** Grain size analysis example at upstream.

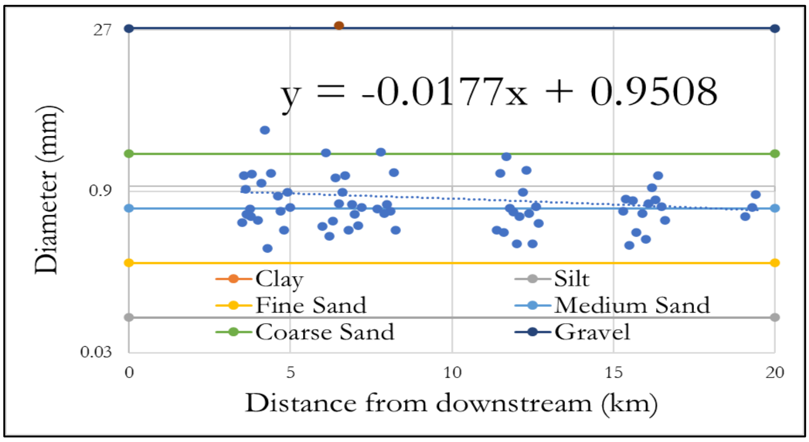


**Figure 9.** L2 mean grain size and soil type ($D_{50}$).

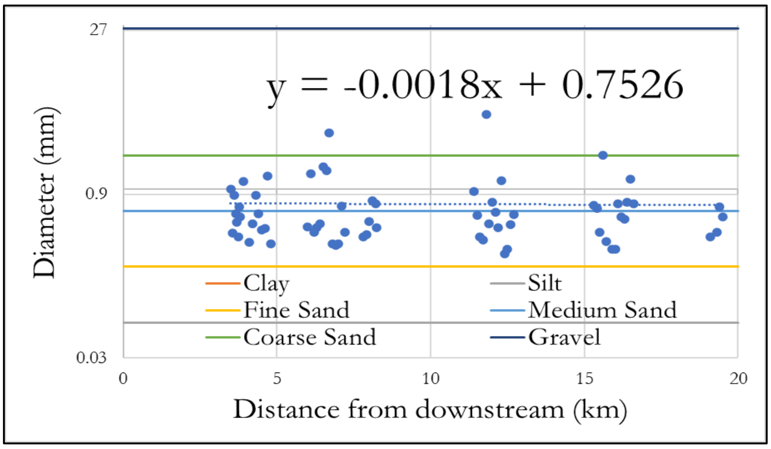


**Figure 10.** L1 mean grain size and soil type ($D_{50}$).

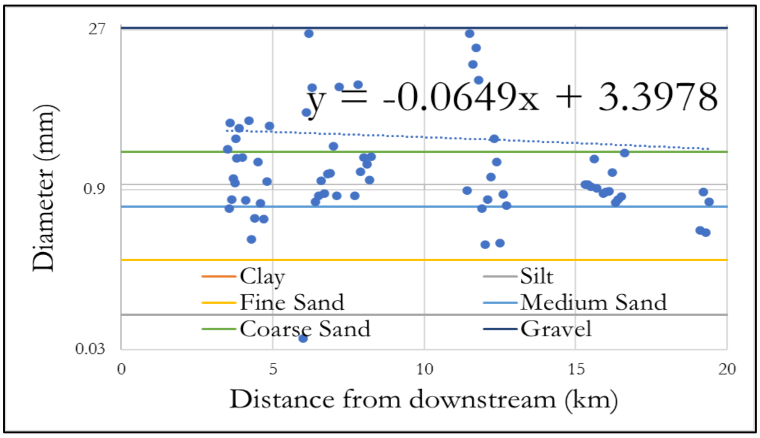


**Figure 11.** C mean grain size and soil type ($D_{50}$).

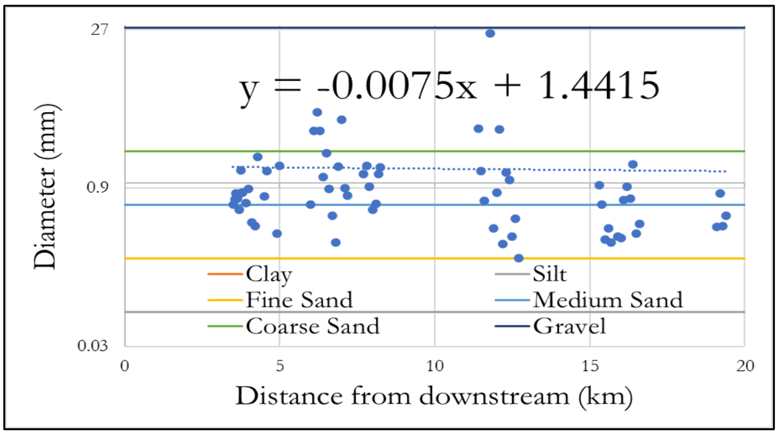


**Figure 12.** R1 mean grain size and soil type ($D_{50}$).

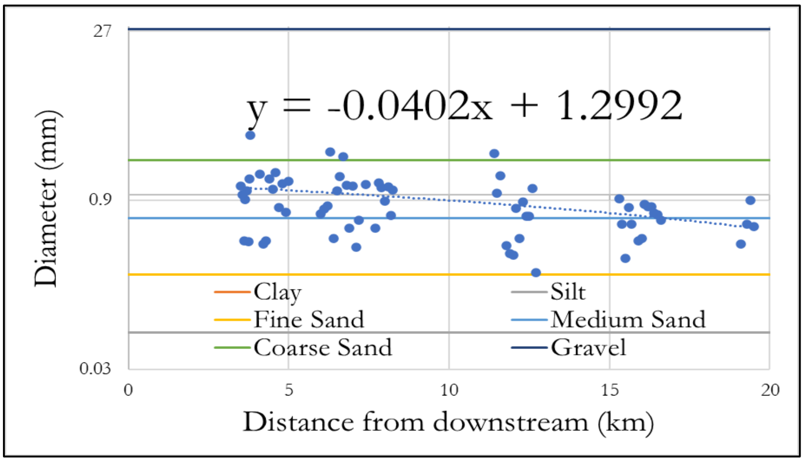


**Figure 13.** R2 mean grain size and soil type ($D_{50}$).

**Table 4.** Averaged mean grain diameter and soil type.

| **Pre-Interp. Averaged Mean Bed Diameter (mm)** | | | | | |
|---|---|---|---|---|---|
| Spots | L2 | L1 | C | R1 | R2 |
| D50 | 0.78 | 0.74 | 2.74 | 1.36 | 0.91 |
| Soil Type | Coarse Sand | Coarse Sand | Gravel | Coarse Sand | Coarse Sand |

### 4.2 Bankfull Discharge Calculation

Using Eq. (6, 7) following what Fig. 6 illustrates, the result of wetted areas can be seen in Table 5 and are used for calculating bankfull discharge with results as shown in Table 6.

**Table 5.** Wetted area statistics.

| **Data** | **Wetted Areas ($m^2$)** | | | | | |
|---|---|---|---|---|---|---|
| | **Re1** | **Re2** | **Re3** | **Re4** | **Re5** | **Re6** |
| Max | 37.1 | 113.2 | 223.9 | 171.5 | 220.1 | 40.5 |
| Avg | 15.6 | 34.7 | 67.8 | 100.0 | 48.0 | 29.6 |
| St.Dev | 8.3 | 28.4 | 46.2 | 56.4 | 39.1 | 15.4 |
| Var | 0.5 | 0.8 | 0.7 | 0.6 | 0.8 | 0.5 |

**Table 6.** Bankfull discharge statistics.

| **Data** | **Bankfull Discharges ($m^3/s$)** | | | | | |
|---|---|---|---|---|---|---|
| | **Re1** | **Re2** | **Re3** | **Re4** | **Re5** | **Re6** |
| Max | 15.4 | 324.8 | 1078.9 | 917.7 | 989.4 | 183.7 |
| Avg | 5.8 | 33.8 | 169.3 | 484.5 | 95.9 | 127.1 |
| St.Dev | 4.3 | 57.8 | 229.8 | 350.3 | 168.7 | 59.9 |
| Var | 0.7 | 1.7 | 1.4 | 0.7 | 1.8 | 0.5 |

### 4.3 Grain Size Interpolation ($D_{50}$)

As to what had been explained in **Sub-unit 3.3**, there is a need to fill blank soil samples by three different approaches. The equations used in the Linear Interpolation are the trendline equations in Fig. 9-13, and the Shear Stress Correlation Interpolation uses the equations in Fig. 14-18. Table 7-8 show the equations' recapitulation for both methods, with *y* being $D_{50}$ and *x* being cross-section distance from downstream.

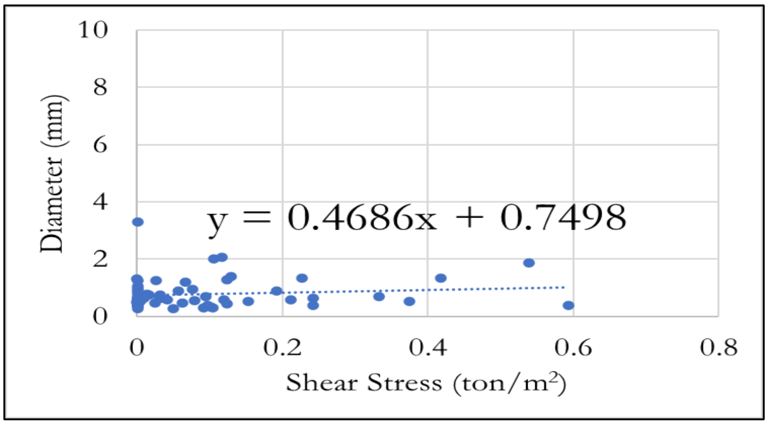


**Figure 14.** L2 shear stress and $D_{50}$ relation.

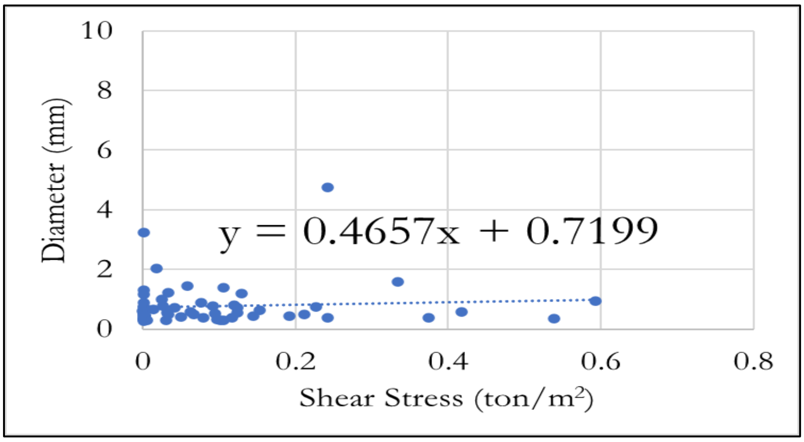


**Figure 15.** L1 shear stress and $D_{50}$ relation.

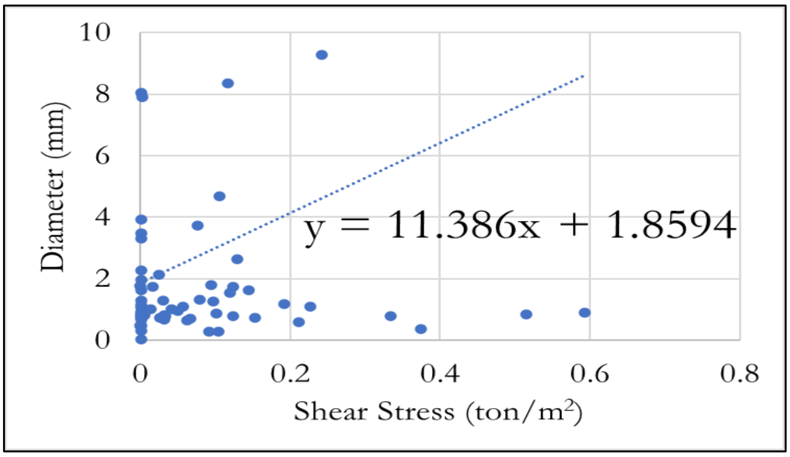


**Figure 16.** C shear stress and $D_{50}$ relation.

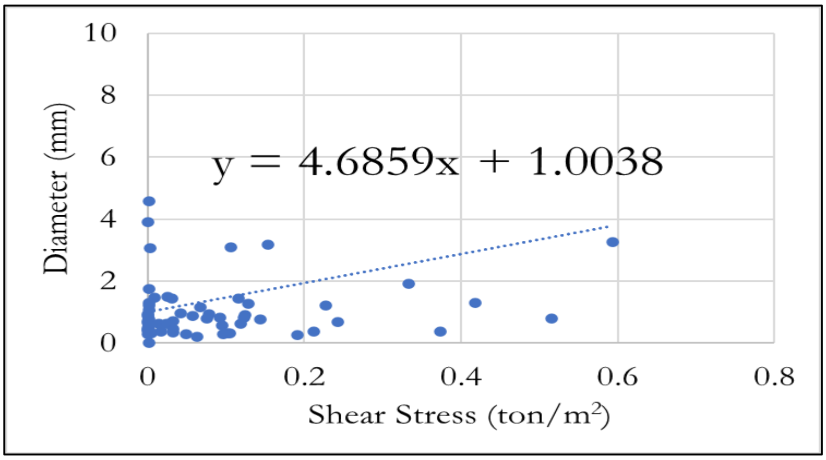


**Figure 17.** R1 shear stress and $D_{50}$ relation.

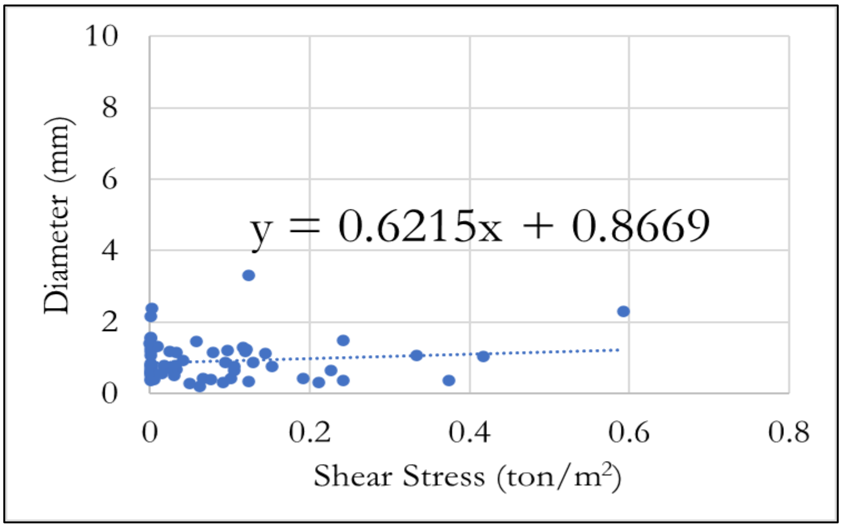


**Figure 18.** R2 shear stress and $D_{50}$ relation.

**Table 7.** Trendline equation of $D_{50}$ to station.

| L2 | L1 | C | R1 | R2 |
|---|---|---|---|---|
| y= - 0.0177x + 0.9508 | y= - 0.0018x + 0.7526 | y= - 0.0649x + 3.3978 | y= - 0.0075x + 1.4415 | y= - 0.0402x + 1.2992 |

**Table 8.** Trendline equation of $D_{50}$ to shear stress.

| L2 | L1 | C | R1 | R2 |
|---|---|---|---|---|
| y= 0.4686x + 0.7498 | y= 0.4657x + 0.7199 | y= 11.386x + 1.8594 | y= 4.6859x + 1.0038 | y= 0.6215x + 0.8669 |

All three methods show different characteristics in filling the unobserved data as shown in the example of center soil spot in Fig. 19-21. To choose which has the best result, an error test is done in the range of P11.4-P12.7 by comparing the interpolation results to fields' samples using error-checking methods (RMSE, MAD, and MAPE). The result is shown in Table 9, with the Forecast Interpolation method being selected. Post interpolation data shows changes in averaged center spot soil type, going from gravel to coarse sand (Table 10).

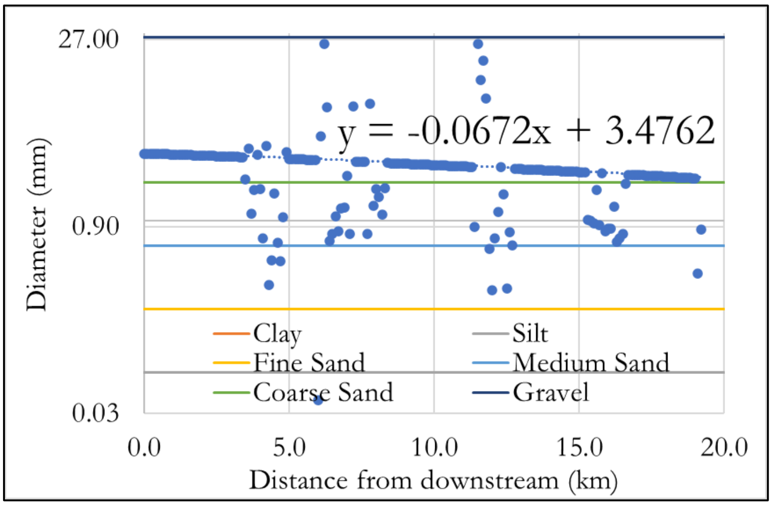


**Figure 19.** $D_{50}$ interpolation with linear interpolation.

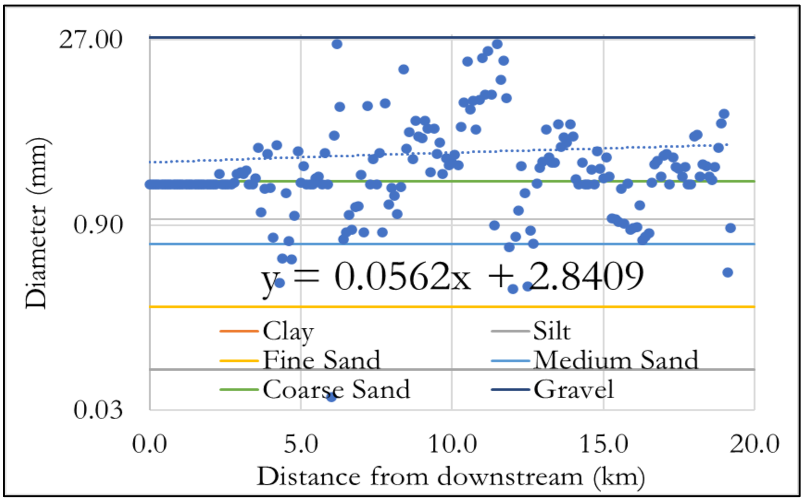


**Figure 20.** $D_{50}$ interpolation with forecast interpolation.

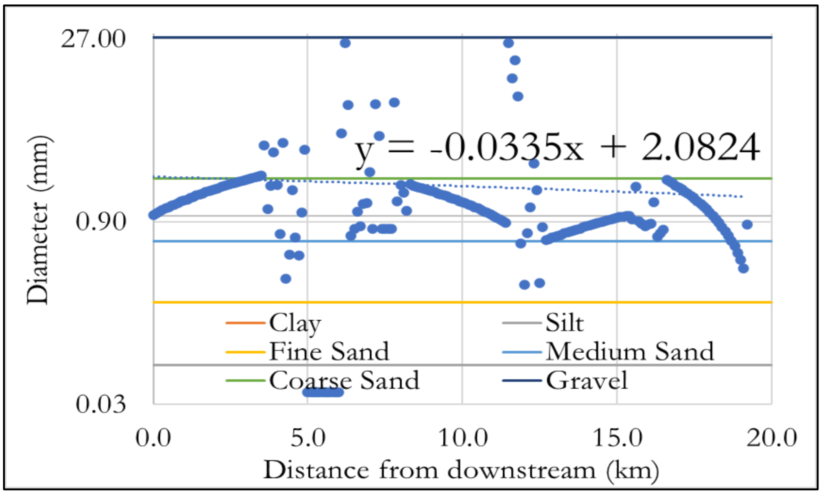


**Figure 21.** $D_{50}$ interpolation with the shear stress correlation interpolation.

**Table 9**. $D_{50}$ interpolations error checking recapitulation.

| **Methods** | **RMSE** | **MAD** | **MAPE** |
|---|---|---|---|
| Linear | 3.33 | 1.77 | 1.20 |
| Forecast | 3.48 | 1.70 | 0.79 |
| Shear Stress | 3.06 | 1.75 | 1.45 |

**Table 10.** Averaged mean soil diameter and soil type post-data filling with interpolation.

| **Post-Interp. Averaged Mean Bed Diameter (mm)** | | | | | |
|---|---|---|---|---|---|
| Spots | L2 | L1 | C | R1 | R2 |
| $D_{50}$ | 0.63 | 0.72 | 1.76 | 1.25 | 0.98 |
| Soil Type | Coarse Sand | Coarse Sand | Coarse sand | Coarse Sand | Coarse Sand |

## 4.4 Regime Dimensioning

Though it is difficult to reach a regime state, each dimension has a chance to be in a state close to its regime potential. By comparing the current state's dimension to seven other regime methods, the results are as in the tables follow. For width, Hey&Thorne becomes the closest method to the current state (Table 11). While for depth and slope, it's Kellerhals (Table 12 and 13).

**Table 11.** Present and regime state comparison for width.

| **Width (w)** | | | |
|---|---|---|---|
| **Methods** | **RMSE** | **MAD** | **MAPE** |
| Griffiths | 40.692 | 24.551 | 72% |
| **Hey&Thorne** | **19.596** | **15.248** | **47%** |
| Generalized Regime | 21.612 | 16.711 | 51% |
| Lacey | 19.818 | 15.606 | 48% |
| Blench | 26.997 | 23.605 | 74% |
| Process-Based Regime | 26.452 | 23.184 | 73% |
| Kellerhals | 23.377 | 19.592 | 62% |

**Table 12.** Present and regime state comparison for depth.

| **Depth (d)** | | | |
|---|---|---|---|
| **Methods** | **RMSE** | **MAD** | **MAPE** |
| Griffiths | 1.857 | 1.605 | 59% |
| Hey&Thorne | 2.169 | 1.841 | 66% |
| Generalized Regime | 10.978 | 6.587 | 189% |
| Lacey | 1.525 | 1.296 | 48% |
| Blench | 8.012 | 6.231 | 241% |
| Process-Based Regime | 2.393 | 1.821 | 69% |
| **Kellerhals** | **1.227** | **1.001** | **38%** |

**Table 13.** Present and regime state comparison for slope.

| Slope (S) | | | |
|---|---|---|---|
| **Methods** | **RMSE** | **MAD** | **MAPE** |
| Griffiths | 0.018 | 0.012 | 417% |
| Hey&Thorne | **0.017** | **0.010** | 268% |
| Generalized Regime | 0.018 | 0.011 | 213% |
| Lacey | **0.017** | **0.010** | 171% |
| Blench | 0.018 | 0.011 | 99% |
| **Kellerhals** | 0.018 | 0.011 | **93%** |

To predict the changes and developments of the channel's size and shape, knowing the present-day state comparison to the regime methods is crucial. The analyses are as follows:

(1) Referring to the width comparison, Hey&Thorne is the closest state to the current one. By this method and MAPE, the width will still have a 47% chance of changes in the future.

(2) Referring to depth and slope comparison, Kellerhals is the closest state to the current one. By this method and MAPE, depth will still have a 38% chance and slope will have a 93% chance of changes in the future.

### 4.5 Average Regime to Present State Comparison

After calculating the regime dimension for each cross-section with seven methods listed in Table 6, the average is obtained by assuming all those methods have the same weight, meaning by dividing the sums by their counts. The comparison for each dimension can be seen in the Fig. 22-24. For width and depth, a number smaller than the regime dimension is considered unstable, but it is the other way around for slope. Although most of the sections have an "unstable" dimension according to the regime state as shown in Table 14, **Sub-unit 4.5** will compare every situation by quantifying them through ratios.

**Table 14.** Percentage of unstable cross sections.

| Unstable Cross Sections (%) | | |
|---|---|---|
| Width | Depth | Slope |
| 17% | 88% | 64% |

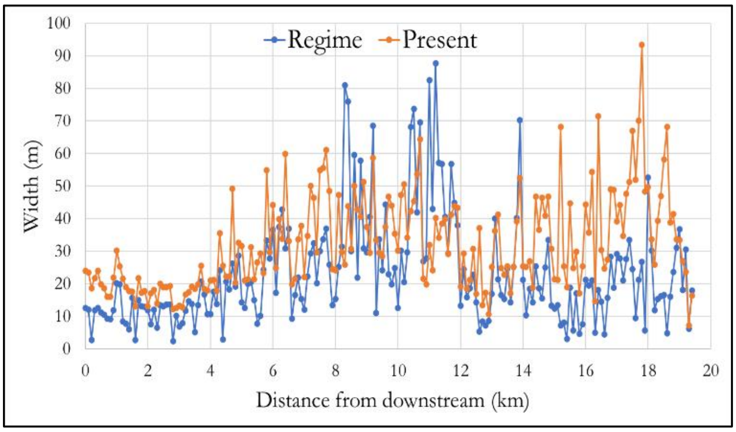


**Figure 22.** Current and regime state comparison in width in long-sectional view.

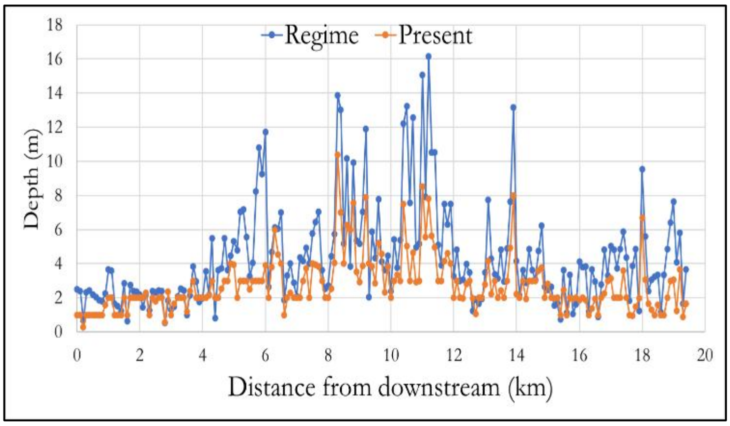


**Figure 23.** Current and regime state comparison in depth in long-sectional view.

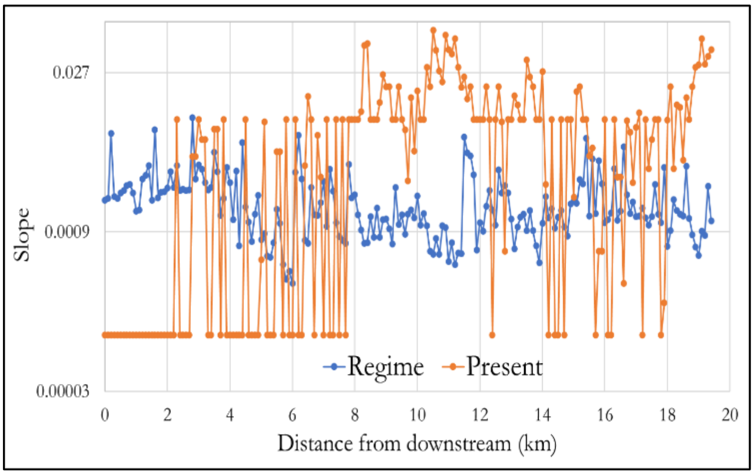


**Figure 24.** Current and regime state comparison in slope in long-sectional view.

### 4.6 Regime Ratio

The regime ratio is obtained by dividing the present state dimension, or as resistance, to the regime state dimension, or as load. This ratio is often considered as Safety Factor (SF), with the results as follows:

**Table 15.** Regime ratio recapitulation in each river slope classification.

| **Regime Ratio** | | | |
|---|---|---|---|
| River Classification | Width (w) | Depth (d) | Slope (S) |
| Re6 | 1.08 | 0.48 | 0.03 |
| Re5 | 2.37 | 0.71 | 2.38 |
| Re4 | 0.74 | 0.52 | 0.02 |
| Re3 | 1.52 | 0.74 | 3.04 |
| Re2 | 1.80 | 0.79 | 11.81 |
| Re1 | 2.12 | 0.70 | 27.04 |

Another step in the analysis is to average all the ratios obtained into a single number that can represent cross-sectional situations to regime concepts. It is not as simple as averaging the dimensions as these three parameters have their weights regarding their impact on river morphologic changes. Papanicolaou in 2010 [26] did a study about quantifying the relative importance of the channel's dimensions that generate river morphology and sediment transport. The study concludes that width becomes the most influential variable, followed by slope and depth. Based on it, the averaged regime ratio is shown as follows:

**Table 16.** Averaged regime ratio recapitulation in each river slope classification.

| **Averaged Regime Ratio** | |
|---|---|
| River Classification | Average |
| Re6 | 0.65 |
| Re5 | 2.04 |
| Re4 | 0.48 |
| Re3 | 1.82 |
| Re2 | 4.60 |
| Re1 | 9.31 |

### 4.7 Regime Ratio on Slope Classification

First, **Sub-unit 4.5** provides how different slope classes would correlate with the results of regime ratios. The graph below shows the relation of slopes in low to high order. The graph shows that river sections with lower slopes (downstream) have a greater regime ratio as they should, and would go less as the slope increases. While for width and depth, it is randomized and have no specific likeliness in trends. The graph also illustrates the relation between slope and averaged regime ratio, and it shows the same correlation as what slope has.

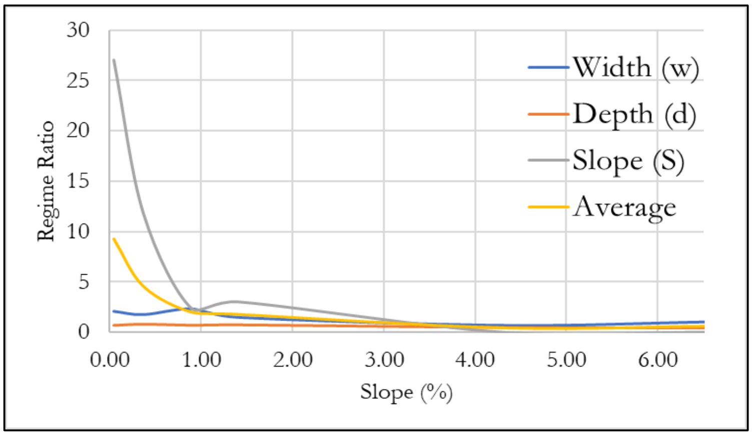


**Figure 25.** Slope relation to regime ratios.

Second, the table below shows the averaged regime ratios from a representation of one, three, and five in each river class, compared to Table 16 with a data density of 100 meters. The result shows that the use of three points at most upstream, middle stream, and most downstream (UMD) has an error percentage of 12.49%. The best result is shown in the representation of three samples in each river class, as Fig. 26 shows.

**Table 17.** The comparison of minimum data density

| **River Classification** | **Averaged Regime Ratio** | | | | |
|---|---|---|---|---|---|
| | **Per 100m** | **UMD** | **1** | **3** | **5** |
| R6 | 0.6 | - | 0.5 | 0.6 | 0.6 |
| R5 | 2.0 | - | 1.0 | 0.6 | 0.7 |
| R4 | 0.5 | - | 0.5 | 0.5 | 0.5 |
| R3 | 1.8 | - | 0.4 | 0.8 | 1.3 |
| R2 | 4.6 | - | 23.2 | 8.4 | 7.0 |
| R1 | 9.3 | - | 5.1 | 6.4 | 6.7 |
| Average | 3.1 | 2.8 | 5.1 | 2.9 | 2.8 |
| Error Percentage (%) | | 12% | 62% | **8%** | 11% |

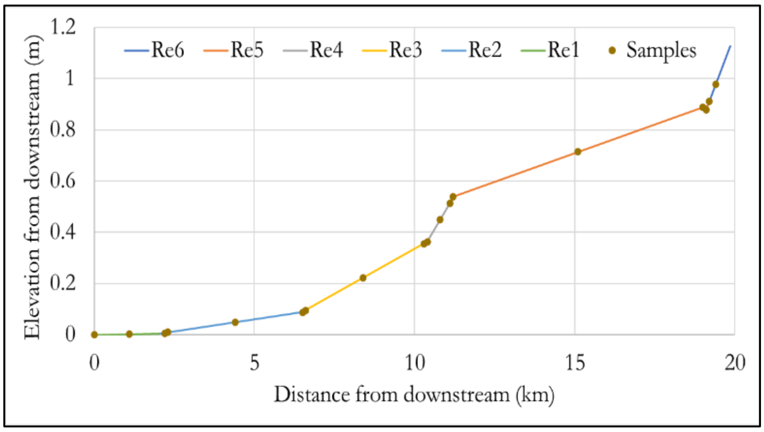


**Figure 26.** Three representations's locations per river slope classification in long section.

### 4.8 Regime Curve

The regime curve is obtained by the averages in **Sub-unit 4.5**, and be visualized into graphs by the dimensions' relation to dominant flow ($m^3/s$). These curves are meant to deliver easy information to be used to analyze the river's present state from its dominant discharge. For example, in a sampled cross-section with a certain number of bankfull discharges, the minimum regime dimension will be right on the curve. If the current state's dimension is higher (or lower for slope), it means it has reached its regime state. The curves for each dimension are as follows, with Table 18 showing the trendline equations for them.

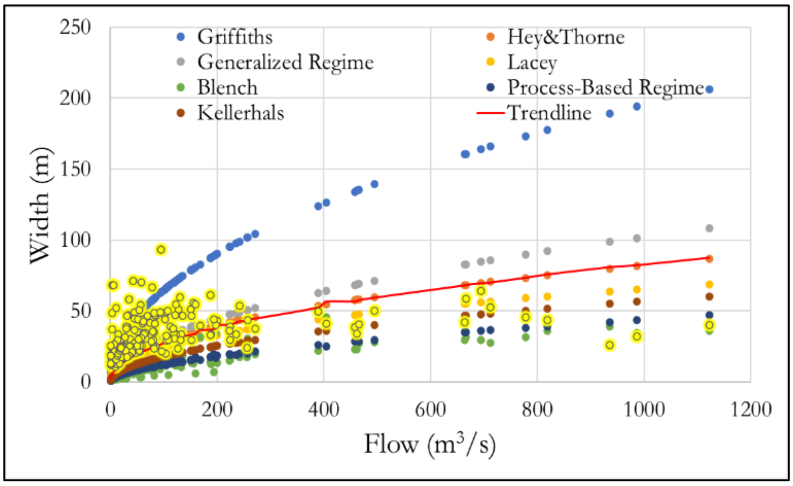


**Figure 27.** Width regime curve.

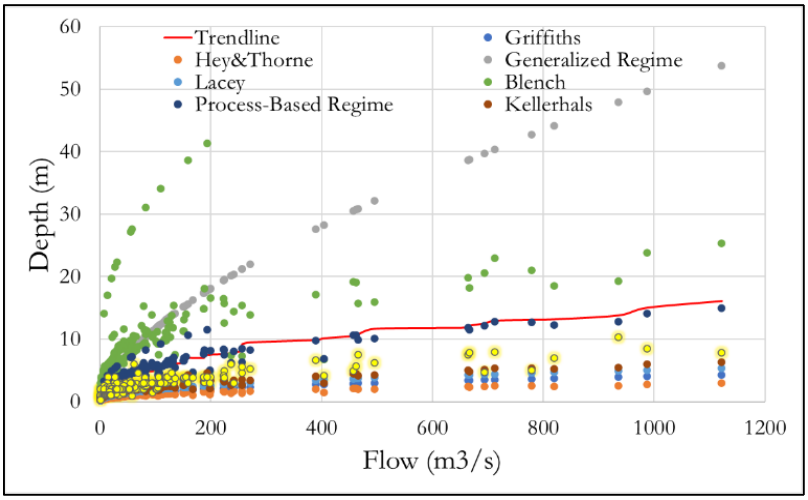


**Figure 28.** Depth regime curve.

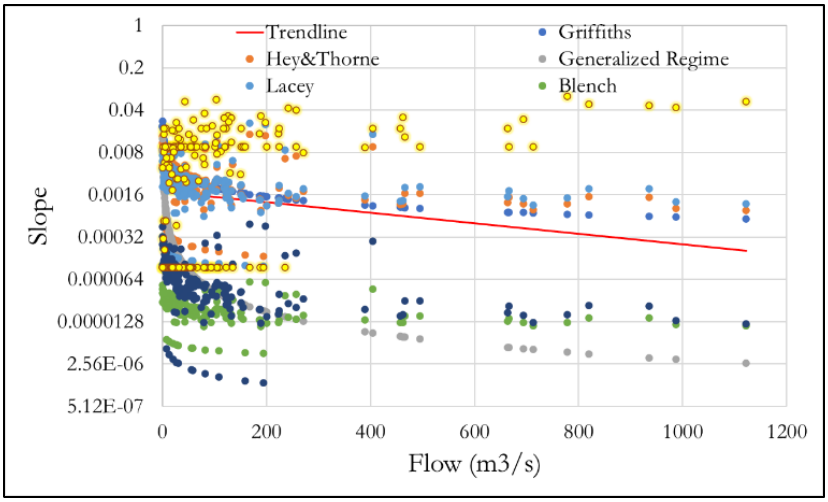


**Figure 29.** Slope regime curve.

**Table 18.** Trendline equation between flow and regime dimension in regime curve.

| **Equation Between Flow and Regime Dimension** | | |
|---|---|---|
| Width | Depth | Slope |
| $w = 10^{-5}Q^2 + 0.154Q + 10.064$ | $d = 10^{-5}Q^2 + 0.029Q + 2.055$ | $S = 0.0018\ e^{-0.002Q}$ |

### 4.9 Soil Finer Percentages Comparison

Though some regime methods mention the use of mean diameter grain size in the dimensioning, some others do not. This part of analysis is meant to compare the result of finer percentages' alternatives, from $D_{50}$ to $D_{30}$ and $D_{70}$ in Fig. 7. The results are as shown as follow:

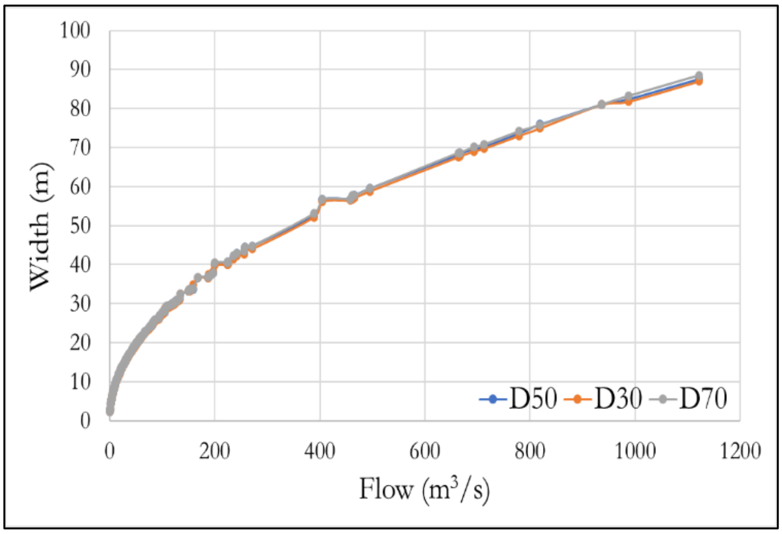


**Figure 30.** Width regime curve in three different finer percentages.

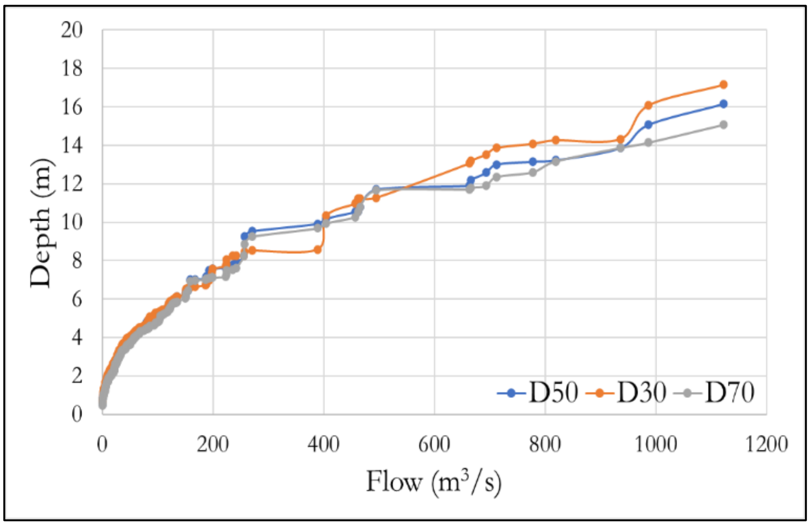


**Figure 31.** Depth regime curve in three different finer percentages.

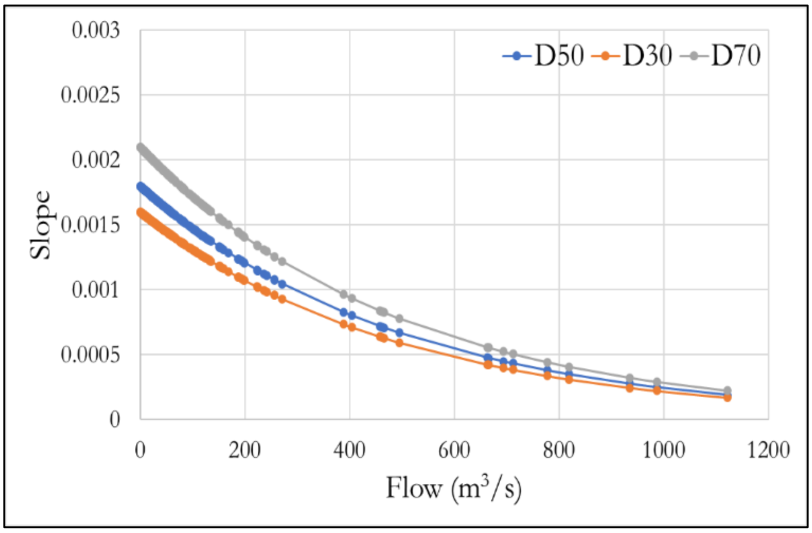


**Figure 32.** Slope regime curve in three different finer percentages.

**Table 19.** Regime curve error tests by changing finer percentages compared to $D_{50}$.

| Dimension | Spot | Error Tests | | |
|---|---|---|---|---|
| | | **RMSE** | **MAD** | **MAPE** |
| Width | $D_{30}$ | 0.25 | 0.17 | 0.72% |
| | $D_{70}$ | 0.17 | 0.10 | 0.47% |
| Depth | $D_{30}$ | 0.31 | 0.22 | 5.71% |
| | $D_{70}$ | 0.22 | 0.16 | 4.50% |
| Slope | $D_{30}$ | 0.0002 | 0.0002 | 11.11% |
| | $D_{70}$ | 0.0003 | 0.0003 | 16.67% |

Based on the results above, it is shown that dimensioning width regime has the lowest error percentage of MAPE by an average of 0.59%, followed by depth at 5.11% and slope at 13.89%. The main analysis in this part is not about how different it is, but how it affects the dimensioning. Concluding, width and slope have a directly proportional relation to finer percentages, while depth is reversely proportional.

### 4.10 Soil Specimen Spots Comparison

Some regime methods mention the use of bed samples in the dimensioning, while others do not. This part of analysis is meant to compare the results of spots' alternatives, or L1 and R1 in Fig. 4, in the condition where the C spot is not accessible in site visits. The results are as shown as follow:

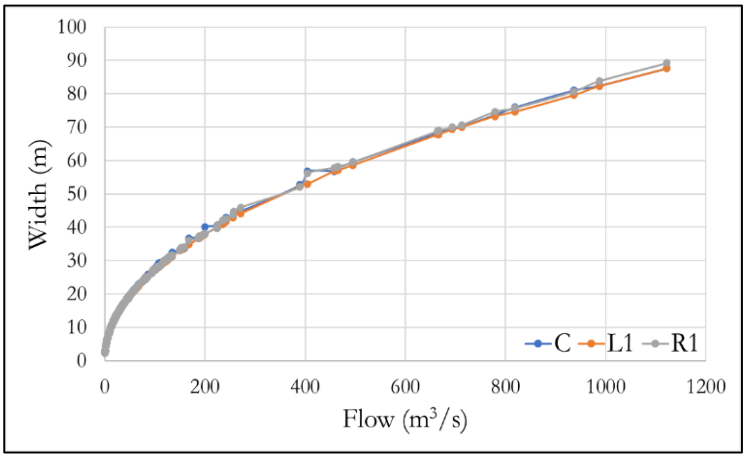


**Figure 33.** Width regime curve in three different soil specimen spots.

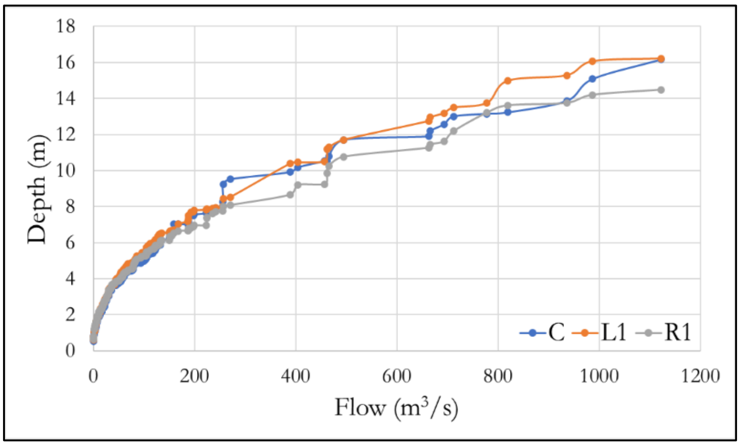


**Figure 34.** Depth regime curve in three different soil specimen spots.

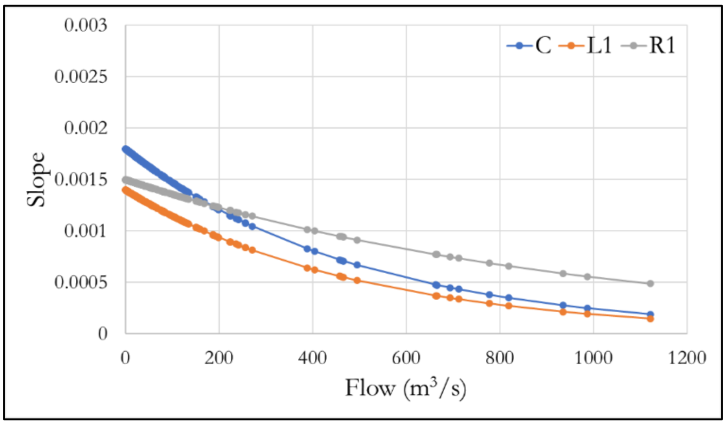


**Figure 35.** Slope regime curve in three different soil specimen spots.

**Table 20.** Regime curve error tests by soil specimen spots compared to center specimen spot.

| **Dimension** | **Spot** | **Error Tests** | | |
|---|---|---|---|---|
| | | **RMSE** | **MAD** | **MAPE** |
| Width | L1 | 0.45 | 0.22 | 0.82% |
| | R1 | 0.34 | 0.20 | 0.82% |
| Depth | L1 | 0.35 | 0.26 | 6.54% |
| | R1 | 0.34 | 0.22 | 5.55% |
| Slope | L1 | 0.0003 | 0.0003 | 22.22% |
| | R1 | 0.0002 | 0.0002 | 16.05% |

Based on the results above, it is shown that **moving soil specimen spots** to the left and/or right (from C to L1 or R1) is allowed only for dimensioning **width** regime by an average MAPE of 0.82%. For depth and slope, it is kind of tricky as depth has an average MAPE of 6.05% and slope of 19.14%. The risk of inaccuracy is left to the user to decide.

## 5. Conclusion and Recommendation

### 5.1 Conclusion

The conclusions from the results and discussions above are as follows:

(1) The best way to fill the soil data gap information in unobserved locations is to **interpolate data between two known observed data**. This method is strengthened as HEC-RAS [25] also uses it in its sediment modeling.

(2) Although a regime state is difficult to reach, a river's current state's dimension is most likely to be similar to one or more regime methods. As for Plumbon River, width-wise is close to Kellerhals with a 47% chance of development, while slope and depth-wise is close to Hey&Thorne with a 38% and 93% chance of development.

(3) The width becomes the dimension with the least unstable, followed by slope and depth for the current and regime state.

(4) The quantification of how a current state's dimensions compare to the regime state's dimensions is done with regime ratio or Safety Factor (SF) by dividing factual to regime dimension. **Any number above 1 is considered stable, and vice versa**. Although being in the same classification of unstable, the number produced can be used to compare one harsher condition to the others.

(5) The **regime curves deliver easy information** to be used to analyze the river's present state from its dominant discharge. By knowing the certain number of bankfull discharges in a studied channel, it is possible to know its comparison to

the regime state by referring only to the regime curves. The problem with these study's curves is they might be **only applicable in Plumbon River**.

(6) For averaged regime ratios, river slope classification has a directly proportional relation to it. While for width and depth, it is randomized and do not show any likeliness in trends.

(7) In substituting sample data needed for analysis, **three representations per each river slope classification** results best compared to this study's highest density (per 100 meters).

(8) By changing the finer percentage from $D_{50}$ to $D_{30}$ and $D_{70}$, the comparison shows that width and slope are directly proportional to grain size, while depth is reversely proportional. The error compared to $D_{50}$ is an average **MAPE of 6.53%** with width having the least error, followed by depth and slope.

(9) If the site's situation does not allow access to the middle of the bed, **moving spots a bit to the left and/or right** while still being inside the bank stations are allowed **only for regime width dimensioning** (average MAPE of 0.82%). Depth and slope have an average MAPE of 6.05% and 19.14%, concluding it does not recommend the use of L1 and/or R1 for depth and slope regime dimensioning.

### 5.2 Recommendation

The recommendations that could be given from this study for further developments are as follows:

(1) The wetted areas' validity from HEC-RAS has not been verified and is recommended to be compared using software specializing in geometrical drawing such as AutoCAD.

(2) Regime methods used in this study have not been filtered to fit the site's bed soil type after interpolation. Some methods were experimented in graveled beds that fit the pre-interpolated data (Table 4), but did not fit the characteristic of sandy beds after the interpolations (Table 10). For further development, it is recommended to use methods that fit the study case's characteristics.

(3) By the river classification, Re1 is the most downstream part of the river that is greatly affected by tidal waves. Further research on how this location affects regime dimensioning is recommended.

### Acknowledgment

The research team is indebted to Kementerian Pendidikan, Kebudayaan, Riset, dan Teknologi-Direktorat Jenderal Pendidikan Tinggi, Riset, dan Teknologi as the main funder of the study through the program of Program Penelitian dan Pengabdian kepada Masyarakat Tahun Anggaran 2023. Regards, the receiver of funding for NIDN-0027107406.

The research team is also indebted to Laboratorium Teknik dan Pengelolaan Sumber Daya Air, Institut Teknologi Bandung, for the help and contributions in coordinating all the soil samples for sieve analyses.

**Funding:**

This study received financial support from Ministry of Education, Culture, Research and Technology, with contract no: 110/E5/PG.02.00.PL/2023 (June 19th), no: 331/IT1.B07.1/SPP-LPPM/VI/2023 (June 20th), with the research title is Modification of the River Morphological Stability Index (RMSI) as a Determinant of River Reliability.

## References

[1] Julien, P.Y., 2010. Erosion and Sedimentation, 2nd ed. Cambridge University Press, United Kingdom.

[2] Blench, T. (1952). Regime theory for self-formed sediment bearing channels. Transactions, American Society of Civil Engineers, Vol. 117, pp. 383–408Stevens and Nordin, 1987

[3] Stevens, M. A. and Nordin, C. F. (1987). Critique of the regime theory for alluvial channels. Journal of Hydraulic Engineering, Vol. 113, No. 11, pp. 1350–1380.

[4] Wolman, M. G. (1955). The natural channel of Brandywine Creek, Pennsylvania. Geological Survey Professional Paper 271, pp. 1–56, U.S. Department of the Interior, Washington, DC.Ackers, 1992

[5] Ackers, P. (1992). 1992 Gerald Lacey Memorial Lecture: Canal and river regime in theory and practice: 1929–92. Proceedings, Institution of Civil Engineers, Water, Maritime and Energy, Vol. 96, pp. 167–176.

[6] Singh V.P. Handbook of Hydraulic Geometry. 1st ed. United Kingdom: Cambridge University Press; 2022.

[7] Malhotra, (1939). Annual Report (Technical). Central Board of Irrigation, India, 1939–40 (reported in Inglis, 1948).

[8] Ackers, P. (1964). Experiments on small streams in alluvium. Journal of the Hydraulics Division, Vol. 90, No. 4, pp. 1-37.

[9] Blench, T. (1951). Regime theory for self-formed sediment bearing channels. Proceedings, ASCE, Vol. 77, Separate 70, pp. 1-18.

[10] Simons, D. B. and Alberton, M. L. (1963). Uniform water conveyance channels in alluvial material. Transactions, ASCE, Vol. 96, No. HY1, p. 123.

[11] Kondap, D. M. and Garde, R. J. (1979). Design of stable channels. ICOLD Special Issue, Journal of Irrigation and Power, Vol. 36, No. 4, October.

[12] Kellerhals, R. (1967). Stable channel with gravel-paved beds. Journal of

Waterways and Harbors Division, ASCE, Vol. 93, No. WW1, pp. 63-84.

[13] Griffiths, G. A. (1980). Hydraulic geometry relationships of some New Zealand gravel-bed rivers. Journal of Hydrology (New Zealand), Vol. 19, No. 2, pp. 106-118.

[14] Hey, R. D. and Thorne, C. R. (1986). Stable channels with mobile gravel beds. Journal of Hydraulic Engineering, ASCE, Vol. 112, No. 3, pp. 671-689.

[15] Glossary of Termsin River Morphology and Hydraulics. Bankfull discharge [Internet]. Available from: https://www.brrc.unr.edu/education/glossary/bankful-discharge/. Accessed: June 19, 2023.

[16] Nixon, M. (1959). A study of bankfull discharge of rivers in England and Wales. Proceedings, Institution of Civil Engineers, Vol. 12, pp. 157–174.

[17] Inglis, C. C. (1947). Meanders and their bearing in river training. Maritime Paper No. 7, Institution of Civil Engineers, London.

[18] Lacey, G. (1929–1930). Stable channels in alluvium. Proceedings, Institution of Civil Engineers, Vol. 229, pp. 259–384.

[19] Kennedy, R. G. (1895). On the prevention of silting in irrigation canals. Proceedings, Institution of Civil Engineers, Vol. 119, pp. 281–290.

[20] Lacey, G. and Pemberton, W. (1972). A general formula for uniform flow in self-formed alluvial channels. Proceedings, Institution of Civil Engineers, Part 2, Vol. 53, pp. 373–381.

[21] Ackers, P. (1983). Sediment Transport Problems in Irrigation System Design. Developments in Hydraulic Engineering-I, edited by Novak, P., Applied Science Publishers, London, pp. 151–195.

[22] Ackers, P. (1988). Alluvial channel hydraulics. Journal of Hydrology, Vol. 100, pp. 177–204.

[23] Simons, D. B. and Alberton, M. L. (1960). Uniform water conveyance channels in alluvial material. Journal of Hydraulics Division, ASCE, Vol.85, No. HY5, pp. 33–71.

[24] Bakker, B., Vermas, H., and Choudri, A. M. (1986). Regime theories updated or outdated. International Commission on Irrigation and Drainage, Darves Bornoz Special Session, Lahore, Report 9.

[25] Center, H. E. (2016). HEC-RAS River Analysis System. USA: U.S. Army Corps of Engineers.

[26] Papanicolaou, A. N., et al. "Influence of river channel dimensions on flow and sediment transport: a flume study." Earth Surface Processes and Landforms 35.2 (2010): 232-240.

[27] Schumm, S.A., Harvey, M.D. and Watson, C.C. 1984. Incised Channels: Morphology, Dynamics, and Control. Water Resources Publications. Littleton, Colorado. 200 pp.

[28] Thorne, C.R. 1999. Bank processes and channel evolution in the incised rivers of north-central Mississippi (Pgs. 97 – 122) In Darby, S.E. and Simon, A.S. Incised river channels: processes, forms, engineering and management. John Wiley & Sons. Chichester, England.

[29] Slater LJ, Khouakhi A, Wilby RL. River channel conveyance capacity adjusts to modes of climate variability. Scientific Reports. 2019 Sep 2;9(1).

[30] Rosgen D.L. Applied River Morphology. 2nd ed. 1996.

[31] Halim F. APLIKASI METODE KONSEP REGIME PADA PERENCANAAN SUDETAN DI SUNGAI SARIO. Jurnal Ilmiah MEDIA ENGINEERING. 2011;1(1).

[32] Sharma N, Swamee P. Lacey regime equations for river Brahmaputra Mechanics of sediment entrainment View project Flow resistance of large-scale roughness." View project Prabhata K. Swamee Institute of Technology and Management 86 PUBLICATIONS 2,020 CITATIONS SEE PROFILE Lacey regime equations for river Brahmaputra Les équations du régime de Lacey pour le fleuve Brahmaputra. Article in Journal of Hydraulic Research. 2008;46(5):707–10.

[33] Zaw KM. Application of Regime Relationships to Macleay River. 1970.

[34] Hodson TO. Root-mean-square error (RMSE) or mean absolute error (MAE): when to use them or not. Geoscientific Model Development. 2022 Jul 19;15(14):5481–7.

[35] Chai, T. and Draxler, R. R.: Root mean square error (RMSE) or mean absolute error (MAE)? – Arguments against avoiding RMSE in the literature, Geosci. Model Dev., 7, 1247–1250, https://doi.org/10.5194/gmd-7-1247-2014, 2014.

[36] Khair U, Fahmi H, Hakim SA, Rahim R. Forecasting Error Calculation with Mean Absolute Deviation and Mean Absolute Percentage Error. Journal of Physics: Conference Series. 2017 Dec;930:012002.

[37] Y. Moon and T. Yao, "A robust mean absolute deviation model for portfolio optimization,"

Comput. Oper. Res., vol. 38, no. 9, pp. 1251–1258, 2011.

[38] C. Leys, C. Ley, O. Klein, P. Bernard, and L. Licata, "Detecting outliers: Do not use standard deviation around the mean, use absolute deviation around the median," J. Exp. Soc. Psychol., vol. 49, no. 4, pp. 764–766, 2013.

[39] J. McKenzie, "Mean absolute percentage error and bias in economic forecasting," Econ. Lett., vol. 113, no. 3, pp. 259–262, 2011.

[40] A. de Myttenaere, B. Golden, B. Le Grand, and F. Rossi, "Mean Absolute Percentage Error for regression models," Neurocomputing, vol. 192, pp. 38–48, 2016.